Sigma Journal of Engineering and Natural Sciences
Web page info: https://sigma.yildiz.edu.tr
DOI: 10.14744/sigma.2021.00075

Research Article

Discovery of new herbal anthelmintics from *Artemisia Annua L.* via *in silico* molecular docking and *in vivo* extract application

Dilara KARAMAN[1], Oya GİRİŞGİN[2], Ahmet Onur GİRİŞGİN[3,*], Hulusi MALYER[4]

[1]*Graduate School of Natural and Applied Science, Bursa Uludag University, Bursa, 16059, Türkiye*
[2]*Karacabey Vocational School, Bursa Uludag University, Bursa, 16700, Türkiye*
[3]*Department of Parasitology, Bursa Uludag University, Bursa, 16059, Türkiye*
[4]*Department of Biology, Bursa Uludag University, Bursa, 16059, Türkiye*

ARTICLE INFO

Article history
Received: 14 December 2021
Revised: 06 April 2022
Accepted: 07 May 2022

Keywords:
Anthelmintic; Artemisia Annua; Friedelin; In Silico Docking; Stigmasterol

ABSTRACT

One of the most important factors limiting the growth and development of children is gastrointestinal helminths. A conscious anthelmintic herbal cure is a rational approach to establishing a sustainable public health program in the treatment of oxyurid infections that are mostly seen in children, disrupt development, frequently recur and are asymptomatic. This study aims to investigate the molecular mechanisms of the anthelmintic features of *Artemisia annua* L. and to compare the antinematodal effect of *A. annua* L. n-hexane extract with Albendazole (ABZ) in naturally infected mice. For this purpose, *A. annua* L. n-hexane extract was extracted and orally administered to Balb-c mice infected with *Syphacia obvelata* oxyurid species at 300, 600, and 1200 mg/kg doses for seven days. Mice were examined for changes in *S. obvelata* egg numbers on days -7, -1, 1, 3, 5, and 7 by the anal tape method. As a reference drug, ABZ was administered at a dose of 5 mg/kg for three days, and as solvent control, corn oil was given in the same way and time as the extract. Some components of *A. annua* L. were investigated for possible chemical interactions and free energy of binding in *Haemonchus contortus* β-tubulin (Hcβ-tubulin) protein and rat Carnitine Palmitoyltransferase II (RnCPT II) enzyme by *in silico* docking simulations. Stigmasterol and friedelin inhibit the RnCPT II enzyme *in silico* with 9.43 nM and 13.07 nM K_i values, respectively, while not binding to Hcβ-tubulin. Arteannuin-B and scopoletin inhibited both RnCPT II and Hcβ-tubulin. *A. annua* L. n-hexane extract at 1200 mg/kg dose reduced oxyurid eggs by 88% on the 7th day. ABZ caused a 65.58% reduction. As the result, arteannuin-B, scopoletin, stigmasterol and friedelin are worthy of isolation and investigation *in vitro* and *in vivo* in terms of their anthelmintic effect. They can be evaluated as potential anthelmintic molecules.

Cite this article as: Karaman D, Girişgin O, Girişgin AO, Malyer H. Discovery of new herbal anthelmintics from *Artemisia Annua L.* via *in silico* molecular docking and *in vivo* extract application. Sigma J Eng Nat Sci 2024;42(1):198–210.

***Corresponding author.**
*E-mail address: aogirisgin@uludag.edu.tr

This paper was recommended for publication in revised form by Regional Editor Ali Erdoğmuş

Published by Yıldız Technical University Press, İstanbul, Turkey

INTRODUCTION

Helminthic infections still have importance in a world where technology and health services have been developing rapidly. More than one billion people worldwide are infected with at least one helminth species [1]. In particular, in preschool children and people living in regions where sanitation is not adequate frequently repeated infections increase the importance of alternative treatment methods that will replace synthetic drugs. Therefore, the discovery of new anthelmintics possessing fewer side effects is a challenge and vital task. Oxyurid infections repeating frequently and passing via oral transmission are more often seen in children and cause the prevention of growth [2]. It has been estimated that approximately 400 million people are infected with *Enterobius vermicularis* [3]. *Syphacia obvelata* is the helminth parasite that frequently infects laboratory mice [4,5]. Eggs of this species belong to the oxyurid group and have a banana shape with an approximate size of 134 X 36 μm. The life cycle is short and direct. After eggs are released from females, hatching takes 5-20 hours. The prepatent period is 11-15 days. The size of females is 3.5-6 mm and males are 1-1.5 mm [6]. This species can live in both laboratory mice and humans [7].

Qing Hao, which means "green herb" in ancient Chinese [8], is called *Artemisia annua* L. in Latin, "Sweet Annie" in English, and "Peygamber Süpürgesi" in Turkish and has been used for various treatment purposes in different regions of the world for thousands of years. The *Artemisia* genus that belongs to the Asteraceae family has the most extensive distribution worldwide [9]. *A. annua* L. consists of various flavonoids, terpenoids, and coumarins. More than 600 secondary metabolites were identified that could be in this plant [10]. Some of them are artemisinin, deoxyartemisinin, artemisinic acid, arteannuin B, stigmasterol, friedelin and artemetin [11]. *A. annua* L. has anti-hyperlipidemic, anti-plasmodial, anti-convulsant, anti-inflammatory, anti-cholesterolemia [12,13], and antiviral [14] properties. Essential oil of *A. annua* L. was reported to show antibacterial, antifungal [15] and acaricidal [16,17] activities. Currently, the effectiveness of *A. annua* L. against coronavirus has been investigated *in vitro*. It has been understood that this plant prevents the replication of SARS-CoV-2 [18]. Being native to China, this plant has been used in Traditional Chinese Medicine for more than 2000 years to reduce fever [8]. In 1970, after discovering that artemisinin isolated from *A. annua* L. is influential in the treatment of malaria, the plant cared around the world and it has spread to large geographies [18]. The inhibition of artemisinin on the malaria parasite *Plasmodium falciparum* has also been demonstrated *in silico* [19]. *In silico* studies investigating the antimalarial mechanism of artemisinin analogs have also allowed the derivatives of artemisinin to be comprehensively studied [20]. Wormwood (*Artemisia absinthium*) has been used for anthelmintic purposes for about a thousand years. In the light of the information provided in Avicenna's famous Medicine Encyclopedia El Kanun Fit Tıbb (Canon Medicinae), although it has been known for a thousand years that absinthine (probably *A. absinthium* species) eliminates pinworm in babies and wormwood syrup is beneficial against intestinal worms [21], the antinematodal mechanism of action of *A. annua* L. remains unknown. In the study conducted by Cala et al. [22], it was suggested that the artemisinin found in *A. annua* L. is responsible for the antinematodal effect, while the fact that *A. absinthium* species, which does not contain artemisinin, has been known to be antinematodal for a long time suggests the presence of other components that create this effect.

Friedelin is a pentacyclic triterpenoid and a cyclic terpene ketone. This molecule contains oxygen in the 3rd position and methyl groups in positions 4, 4a, 6b, 8a, 11, 11, 12b, and 14a. This molecule, a plant metabolite, acts as a non-narcotic pain reliever, an anti-inflammatory, and an antipyretic [23]. Stigmasterol is a steroid derivative and is found in oils, soybeans, plant seeds, and raw milk [24].

Protein-ligand docking simulations performed with the *in silico* molecular modelling method constitute the first step of drug development studies and provide researchers with data at atomic levels on target-drug interactions. This type of computational experimentation has great importance in reducing the workload in drug development. Many researchers prefer Autodock 4.2 [25] software to predict the pharmacokinetics of drug candidate molecules. Tubulin protein is a known target of broad-spectrum anthelmintics in the benzimidazole group. According to the literature, Carnitine Palmitoyl Transferase II (CPT II) enzyme is one of the enzymes seen as a "chokepoint" among anthelmintic drug targets. The homolog of this enzyme, which is involved in lipid metabolism, has been successfully used in an *in silico* modelling study to develop an anthelmintic drug [26]. This study aimed to reveal possible chemical interactions by performing *in silico* docking simulations of some compounds estimated to be found in *A. annua* L. with *Haemonchus contortus* β-tubulin protein and rat Carnitine Palmitoyl Transferase II enzyme. It was also aimed to demonstrate the anthelmintic effect of *A. annua* L. n-hexane extract on the rate of reducing parasite eggs in naturally infected mice with *S. obvelata*.

MATERIALS AND METHODS

Molecular Docking Experiment

Experimental procedure

While the localizations of herbal ligands in β-tubulin protein and CPT II enzyme were examined according to the key-lock fitting model, docking simulation with AutoDock 4.2 [25] and ADT [27,28] was also carried out. Possible chemical interactions of ligands in the protein binding site were investigated by Discovery Studio (Dassault Systèmes Biovia Inc., 2020) [29]. Docking simulations were generated

using an Asus laptop computer with Intel core processor 2GB RAM installed with Linux OS.

Preparation of proteins

Discovery Studio (Biovia Inc.) software was used for protein preparation. For this purpose, theoretical and crystal structures of proteins were obtained from the Brookhaven Protein Databank (http://www.rcsb.org/pdb). *Haemonchus contortus* β-tubulin protein in a complex with ABZ (PDB code: 1OJ0, theoretical structure) [30] and rat CPT II enzyme (PDB code: 2H4T, resolution: 1.90 Å) [31] were selected. Since the crystalline form of hcβ-tubulin is not available in the database, its theoretical structure was used. All water molecules, non-interacting ions and inhibitors were removed. All hydrogen atoms were added. After minimizing the protein with the fast Dreiding-like force field, the "Clean Geometry" tool was used for final optimization.

Preparation of ligands

Bioactive components that can be found in *A. annua* L. have been investigated in the literature. Nine of these components (artemisinin, artemetin, artemisinic acid, deoxyartemisinin, friedelin, stigmasterol, arteannuin B, scopoletin, and quercetin) were obtained from ZincDataBase [32] in mol2 format and PubChem [33] in SDF format. Herbal ligands in mol2 format were converted to PDBQT format with ADT [27,28] software and those in SDF format with Open Babel [34].

Molecular docking

In the docking simulation of β-tubulin protein, the ligand bound to the protein was chosen as the center. For the CPT II enzyme, the coordinates given by Taylor et al. [26] were used, and the x, y, and z coordinates accepted as center were: 61.752, 72.800, and 52.032, respectively. The protein was accepted as rigid, but the hydrogens were only allowed to be relaxed during their action at the protein's active site. The dielectric constant was set to 10, ionic strength to 0.145, grid box dimensions to 60x60x60, and grid point to 0.375Å. Since the number of rotational bonds was less than 10, the maximum generation number was set to 27000, and the maximum evaluation number was selected as 2500000. The Lamarckian genetic algorithm and Autodock4.2 program were chosen for the docking procedure. The docking simulation was carried out with 20 runs.

ADME estimation

According to the results of docking simulations of the herbal ligands, the ADME (Absorption, Distribution, Metabolism, Excretion) properties of two molecules that had the highest binding affinity were estimated via the SwissADME [35] webserver. A prediction was developed based on computational methods by comparing their ability to pass through the blood-brain barrier, gastrointestinal absorption, and oral bioavailability.

Preparation of plant extract

Arial parts of *A. annua* L. were collected in November 2005 from the Acemler region in Bursa, Türkiye. Plants were identified by Prof. Dr. Hulusi Malyer (Bursa Uludag University, Faculty of Science and Literature, Department of Biology). The plants were air-dried in the shade and then powdered with a grinder. N-hexane was filled into the balloon flask in the Soxhlet device as much as possible. Approximately 90 grams of herbal powder was placed in the extractor after being wrapped in blotter paper. At the end of the extraction, n-hexane was removed with a rotary evaporator. The extract was stored in a polypropylene flask at -20°C (yield: 5% w/w).

***In Vivo* Experiment**

Preparation of experimental animals

Balb-c mice of both sexes (28-40 g) at 1-2 years old were obtained from the Bursa Uludag University Experimental Animal Breeding and Application Center because they are used commonly *in vivo* experiments. The animals were kept in standard polypropylene cages at 20-24°C at 55% relative humidity and fed standard pellets and water as they wanted. Naturally infected experiment animals with *S. obvelata* were selected from 150 mice using perianal cellophane tape and Fülleborn faecal flotation methods. Each group was made up of six animals. All experiments were approved by the Uludag University Experimental Animals Local Ethics Committee (no: 2017-10 / 07).

Parasitology

Infected mice were divided into six groups as four treatment groups and two control groups. Approximately the same number of eggs were selected in each group according to the results of the Fülleborn faecal flotation and anal band methods applied on two different days. Group I was drinking water control, Group II was corn oil solvent control, Group III was positive control with the reference drug Albendazole (ABZ) applied at a 5 mg/kg dose for 3 consecutive days, Group IV, V and VI were groups being given *A. annua* L. n-hexane extract at 300, 600, 1200 mg/kg doses, respectively. *A. annua* L. n-hexane extract was completed to 2 ml volume by solving in corn oil. Corn oil and extract concentrations were applied for seven days, while ABZ was applied for three days orally in the same manner with a steel oesophageal gavage.

Egg count with anal tape

After grouping the mice, the perianal cellophane tape method was used to definitively determine the continuation of *S. obvelata* infection in all mice. To determine the efficiency of the plant extract on the egg numbers, arithmetic means of the parasite eggs obtained from the cellophane band method in each group were compared by calculating the % decrease in the number of eggs. To apply this method, 9 cm of cellophane tape was pressed to the mouse's rectum 10-15 times and adhered to the microscope slide, then the

S. obvelata eggs were counted. This procedure was conducted before the application on the -7th and -1st days and during the application on the 1st, 3rd, 5th and 7th days.

RESULTS AND DISCUSSION

The results of the docking simulations in this study are shown in Table 1.

In the redocking process, we performed to reveal the docking experiment's reliability, the RMSD value was found to be 1.56 Å as a result of the redocking of β-tubulin and its natural ligand Albendazole (also the reference drug in this study). Molecular docking analysis of nine of the selected active compounds gave quite different and interesting results for the *Haemonchus contortus* β-Tubulin protein Hcβ-Tubulin (PDB ID: 1OJ0) and *Rattus norvegicus* Carnitine Palmitoyl Transferase II enzyme RnCPT II (PDB ID: 2H4T). Of these molecules, only arteannuin B and scopoletin had free binding energies (ΔG) below -8 kcal/mol with β-tubulin.

For the CPT II enzyme, ΔG values of six of the nine molecules (artemisinin, deoxyartemisinin, friedelin, arteannuin B, stigmasterol, and scopoletin) were found to be below -8 kcal/mol. Artemisinin, deoxyartemisinin, artemisinic acid, arteannuin B, stigmasterol, friedelin and artemetin had been detected in *A. annua* L. infusion by Zheng (1994) [11]. Although artemisinin had been shown as an effective compound against *Plasmodium falciparum* in silico [19], there was no study using Hcβ-tubulin protein and RnCPT II enzyme in order to examine the antinematodal effect of artemisinin. In this study, even though artemisinin was found a potent antinematodal compound with its -8.99 kcal/mol free energy of binding against the RnCPT II enzyme, stigmasterol and friedelin were predicted as more potent ligands than artemisinin. Although Cala et al. [22] suggested that the artemisinin was responsible for the antinematodal effect of *A. annua*, friedelin and stigmasterol should be searched *in vitro* to detect the most effective compound as an antinematodal inhibitor in *A. annua*. Artemetin, which is estimated to have the lowest affinity for the CPT II enzyme among these molecules, formed a hydrogen bond in the CPT II binding site according to Autodock analysis and made van der Waals interactions with various residues (Figure 1).

The most exciting result in Table 1 is that friedelin and stigmasterol have a very high affinity for the CPT II enzyme (13.07 nM and 9.43 nM, respectively), and the K_i values found with β-tubulin are not calculable. When the DLG files of these molecules were examined, it was seen that they were located in the active site in β-tubulin and the docking simulation was performed correctly (Figure 2 A).

These results show that these two molecules may be the significant molecules responsible for the antinematodal

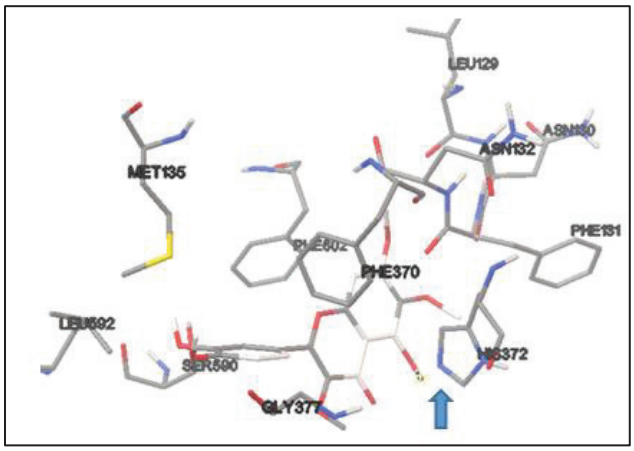

Figure 1. 3D representation of the chemical interactions of the ligand with residues in the binding site as a result of artemetin-CPT II docking simulation. It appears that a hydrogen bond was formed between HIS372 and the H11 atom of artemetin (blue arrow signs).

Table 1. Docking results of selected compounds in *Artemisia annua* L. K_i: Inhibition constant, CPT II: Carnitin Palmitoyl Transferase II

	β-Tubulin		**CPT II**	
Molecule	K_i	ΔG (kcal/mol)	K_i	ΔG(kcal/mol)
Artemisinin	6.37 uM	-7.09	255.16 nM	-8.99
Artemetin	140.87 mM	-1.16	10.75 uM	-6.78
Artemisinic acid	7.38 uM	-7.01	5.59 uM	-7.17
Deoxyartemisinin	2.82 uM	-7.57	476.99 nM	-8.62
Friedelin	-	+72.37	13.07 nM	-10.76
Arteannuin B	14.93 nM	-10.68	170.29 nM	-9.23
Stigmasterol	-	+5.17	9.43 nM	-10.95
Scopoletin	158.57 nM	-9.28	962.70 nM	-8.21
Quercetin	146.93 uM	-5.23	8.53 uM	-6.92

effect of *A. annua* L. and do not inhibit β-tubulin. These results prove that these molecules have another action mechanism than ABZ, providing essential data in predicting the plant's antinematodal mechanism of action.

Friedelin was placed in the binding region of Albendazole in the β-tubulin protein surrounded by side chains of aromatic or polar amino acids. However free energy of binding was found at +72.37 kcal/mol for friedelin. It can be said that the binding region was very narrow for friedelin (Figures 2 B and C). There was enough space for friedelin placement in CPT II for decreasing the energy (Figures 3 A, B, and C).

As for β tubulin, numerous β sheet structures near each other prevented ligand rotation (Figure 2 C). The most striking feature in the placement gives an indication of the entrance cavity of the enzyme. As seen in Figures 3 A and 3 B, the ligand will probably make an entrance from a region where SER488 and PHE370 amino acids were. As shown in Figure 4, when four friedelin rings made strong alkyl interactions with surrounding residues, the 3rd and 5th rings of friedelin in particular made numerous aromatic interactions with PRO133 and HIS372.

Although the distances between rings that interacted with each other were approximately 4-5 Å, five aromatic side chains (PHE370, PRO133, PHE370, HIS372, PHE131) surrounding the ligand thoroughly generated a dense interaction network. Prominently, friedelin's pentacyclic structures made a kind of aromatic sandwich between three different phenyl residues (PHE131, PHE602, and PHE370) by rotating on the 11th carbon plane. When the 5th ring of friedelin entered between PHE602 and PHE131, the 2nd ring of it was in the effects of PHE370 and PHE602 residues (Figure 4 B). As shown in Figure 4 A, both PHE370 and PHE131 performed π-alkyl interactions with methyl groups in the ligand. On the other hand, PHE602 formed aromatic interactions with the 4th and 5th rings while making π-sigma interactions with the 11th methyl group and π-alkyl interactions with the 14th methyl group of the ligand. Other residues that generated van der Waals interactions in the CPT II enzyme's active site with friedelin were ASN130, TYR486, SER488, SER590, LEU592, ALA613, MET135, PHE134, GLY600, GLY601, and GLY377. Of these, SER488, SER590, and LEU 592 applied a stronger force. Among these nine herbal ligands, the molecule with the

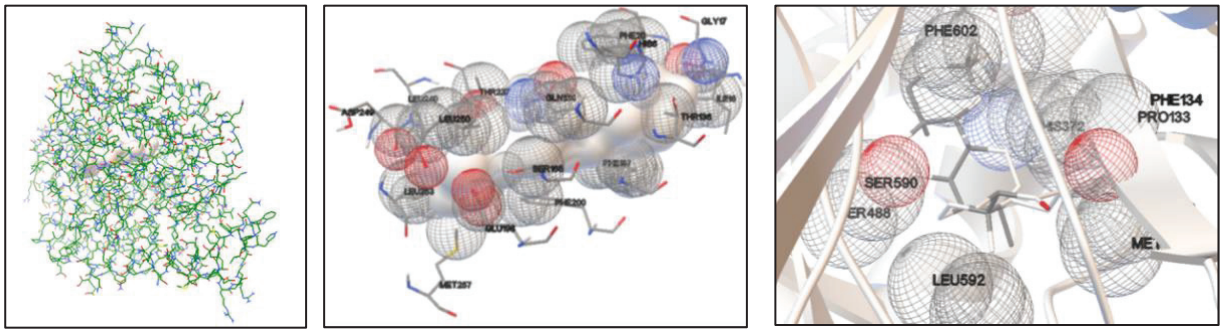

A B C

Figure 2. Interactions between friedelin and β tubulin protein binding site. (A) Opac surface represents friedelin and sticks represent β-tubulin, (B) Friedelin surrounding numerous residues, spheres represent interaction areas of residues, (C) Friedelin is in an intensive interaction area between β-sheets.

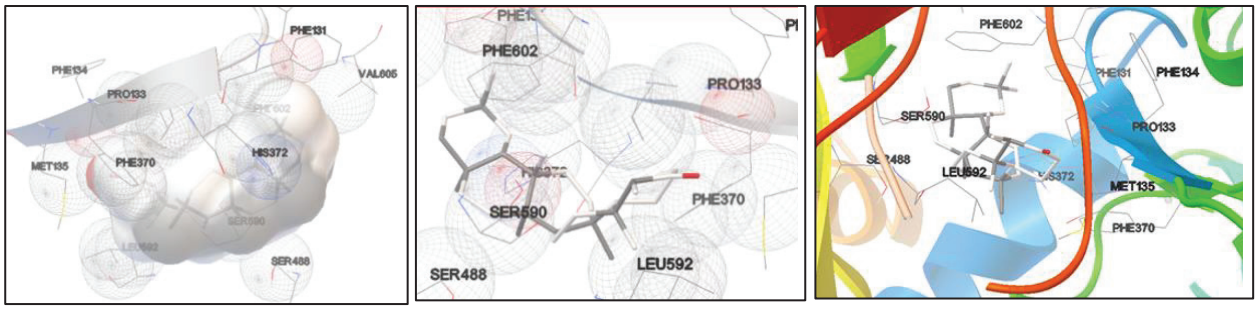

A B C

Figure 3. 3D representations of Friedelin–CPT II interactions (A) Friedelin is shown with surface area style between spheres of side chains. Space is seen between PHE370 and SER488. (B) Friedelin is fitting by rotating in an area comprising aromatic residues. (C) The front loop (red colour) is predicted as a gate to the ligand's entrance.

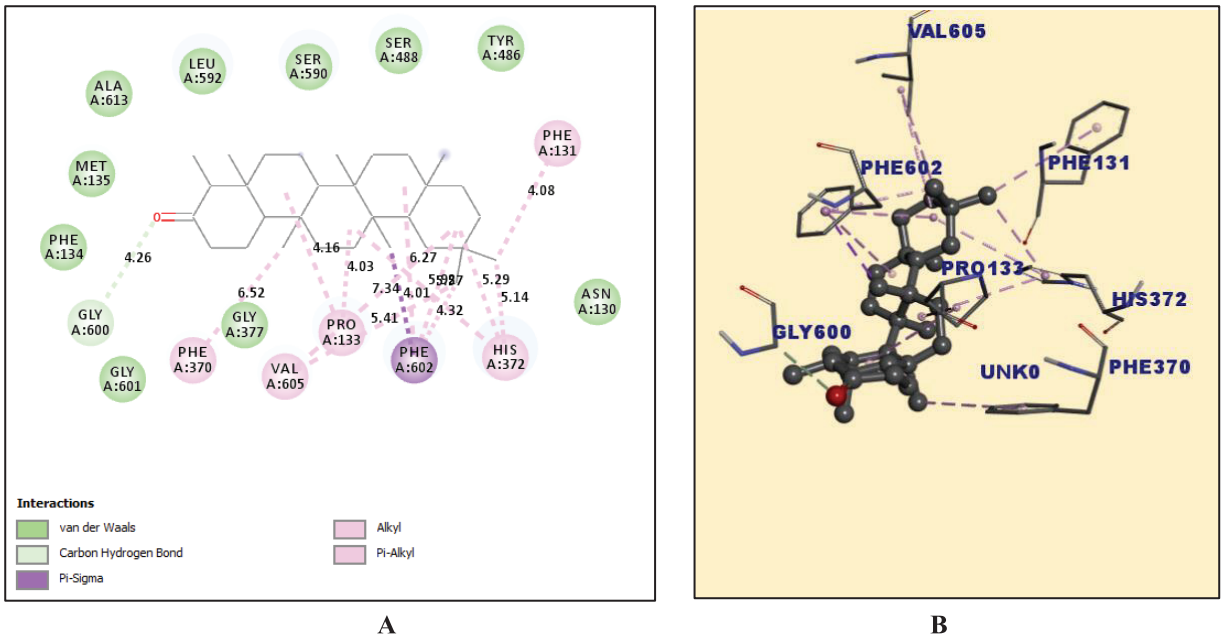

A B

Figure 4. Friedelin interactions with CPT II enzyme. A) 2D representation, distances are given in Å. B) In 3D representation, numerous chemical interactions are seen with very good placement in a cavity surrounded by 3 different phenyl residues (Phe 131, Phe 602 and Phe 370).

highest binding affinity with the CPT II enzyme was found to be stigmasterol with an energy value of -10.95 kcal/mol. Possible interactions of stigmasterol in the CPT II are seen in Figure 5 and Figure 6.

In addition to the tetracyclic nucleus of the molecule, the presence of a bulky group substituted at the cyclopentane ring plays an important role in the insertion of stigmasterol between two parallel α-helices and two perpendicular β-sheets. In stigmasterol, as in friedelin, the central rings made aromatic interactions with residues PHE370, PRO133, and HIS372 (Figure 6A), and HIS372 is again one of the residues closest to the ligand. For friedelin, methyl groups substituted at the central rings are responsible for a significant part of the interactions. In contrast, in stigmasterol, the methyl group in the 1st ring formed an alkyl bond with both PRO133 and HIS37 (Figure 6 A).

The hydroxy group at the 3rd position also made polar interactions with both HIS372 and GLY375 (Figure 6 B).

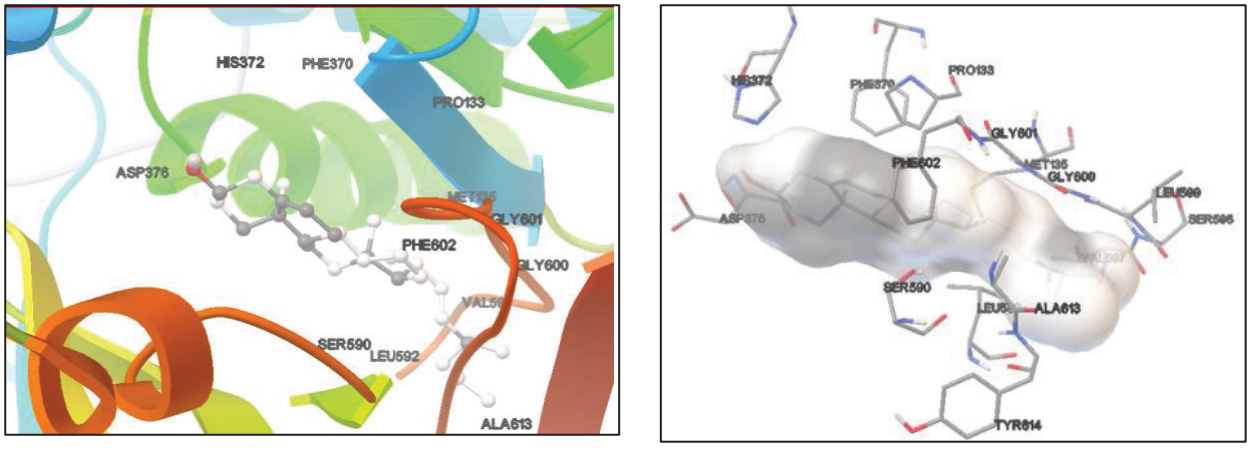

A B

Figure 5. Interactions with stigmasterol in the CPT II enzyme active site. (A) A branched-chain of stigmasterol enters in a loop (red colour) perfectly. (B) Representation of molecular surface for ligand shows the placement of stigmasterol as much as near PHE302, SER 590, ALA613, GLY601, MET135, GLY600, and VAL507.

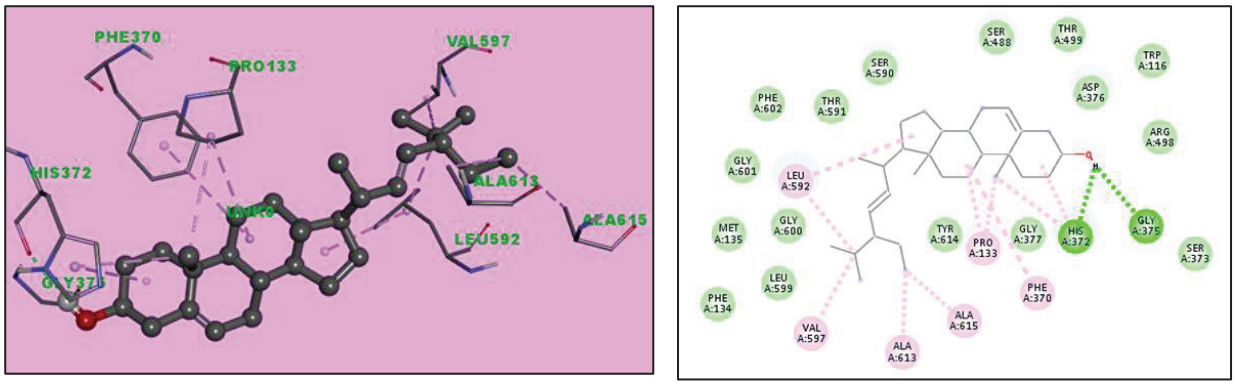

A B

Figure 6. Stigmasterol-CPT II interactions. Imaginary lines represent interactions. A) 3 D and B) 2 D representations. Green lines show van der Waals interactions, pink lines show pi-alkyl interactions.

Arteannuin B (3H-Oxireno (7,8) naphtho (8a, 1-b) furan-3-one, decahydro-7,9a-dimethyl-4-methylene-, (1aR (1aalpha, 1bR *, 4abeta, 7beta, 7abeta, 9aalpha))-); on the other hand, had a higher binding affinity to beta-tubulin unlike artemisinin and deoxyartemisinin (Table 1). For arteannuin B, the ΔG and K_i values calculated with β-tubulin were -10.68 kcal/mol and 14.93nM, respectively, and the same values calculated with CPT II were -9.23 kcal/mol and 170.29 nM, respectively. It can be seen in Figure 8A that the quaternary ring structure of the component and especially the furan ring was important in the placement of arteannuin B in β-tubulin, where the area surrounded by aromatic side-chained amino acids consisted of three phenyls (PHE20, PHE200 and PHE167), two threonines (THR238 and THR 237) and tyrosine (TYR50) residues.

The most important interactions between arteannuin B and β-tubulin shown in Figure 7 are hydrogen bonds forming between the oxygen atoms in the furan ring of arteannuin B and THR238 with a length of 2.02 Å and a length of 2.34 Å between GLN134. It also appears that a π-sigma bond is formed with PHE200 (Figure 7 B). The interactions of arteannuin B with the CPT II enzyme active site are even more interesting (Figures 8 A and B).

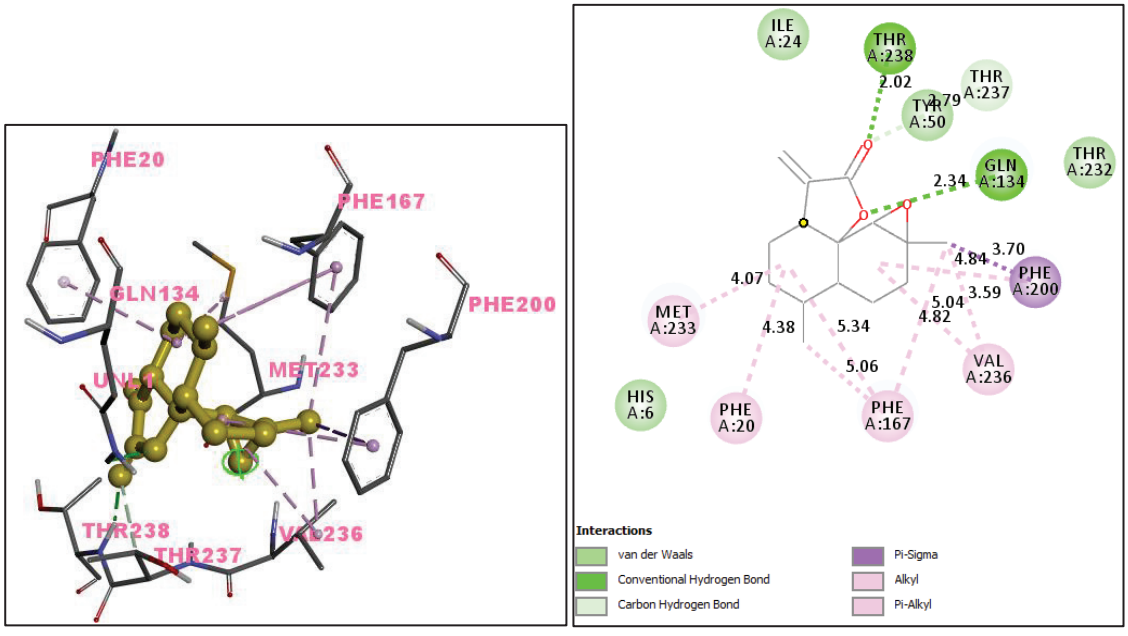

A B

Figure 7. Arteannuin B and β tubulin interactions. A) 3 D representations of predicted chemical interaction. Arteannuin B is represented as yellow colour, and B) 2 D interaction diagrams.

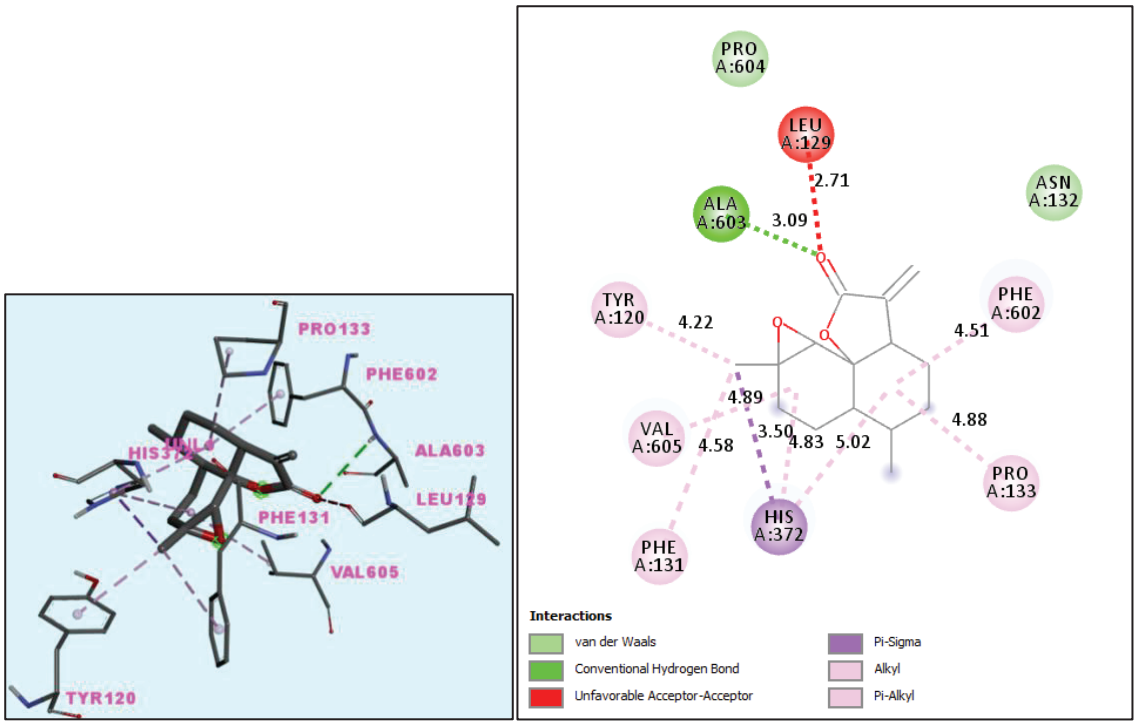

Figure 8. Arteannuin B and CPT II interactions. A) Board stick molecule in center of the image is arteannuin B in 3 D representation, and B) In 2 D representations predicted measure of distances between atoms are shown on lines as Å.

Despite the repulsive force between the oxygen in the carboxylic acid in the LEU329 residue and the oxygen atom at the 3rd position in the component's furan ring, a conventional hydrogen bond formation of approximately 3.09 Å with ALA603 located next to the leucine is shown in Figure 8 B. The aromatic interactions of the molecule with TYR120, PHE131, PHE602, PRO133, and HIS372 led to an increase in the electrostatic attraction force and thus a decrease in the free binding energy in the active area. The SwissADME webserver was used to predict the ADME properties of the two ligands that yielded the best ΔG results. It has been understood that both friedelin and stigmasterol cannot pass through the blood-brain barrier. According to the SwissADME results, Albendazole cannot pass through the blood-brain barrier, but its GI absorption is high. Fridelin and stigmasterol have low GI absorption. In terms of oral bioavailability, friedelin and stigmasterol molecules are found to be suitable for oral ingestion according to Lipinski and Veber's rules, but not according to Ghose, Egan, and Muegge. ABZ is suitable for all in terms of oral bioavailability.

A. annua L. n-hexane extract was used to show the anthelmintic effect on the oxyurid nematodes of naturally infected mice *in vivo*. The arithmetic means of *S. obvelata* eggs were counted on the cellophane band before and during the application. When the changes in the number of parasite eggs by days were examined, astonishing results were encountered. The average number of *S. obvelata* eggs counted in the anal band on the last day of administration was found to be 147 in the mouse group (group V), where *A. annua* L. n-hexane extract was administered at a dose of 600 mg/kg (Table 2).

Table 2. Arithmetic mean of *S. obvelata* eggs counted in cellophane band before and during administration in infected mice

	-7. day	-1. day	1. day	3. day	5. day	7. day
Drinking water	6,4	37,7	2,7	1,9	10,8	10
Corn oil	24,1	29,7	63,1	20,6	10,5	14,6
ABZ	13	24,7	16,2	15	0,5	8,5
A. annua 300 mg/kg	6	24,5	9,3	60,1	25	5,5
A. annua 600 mg/kg	51,7	18,7	32	24,7	112,3	147,9
A. annua 1200 mg/kg	0,3	40	19,3	6,7	2,5	4,8

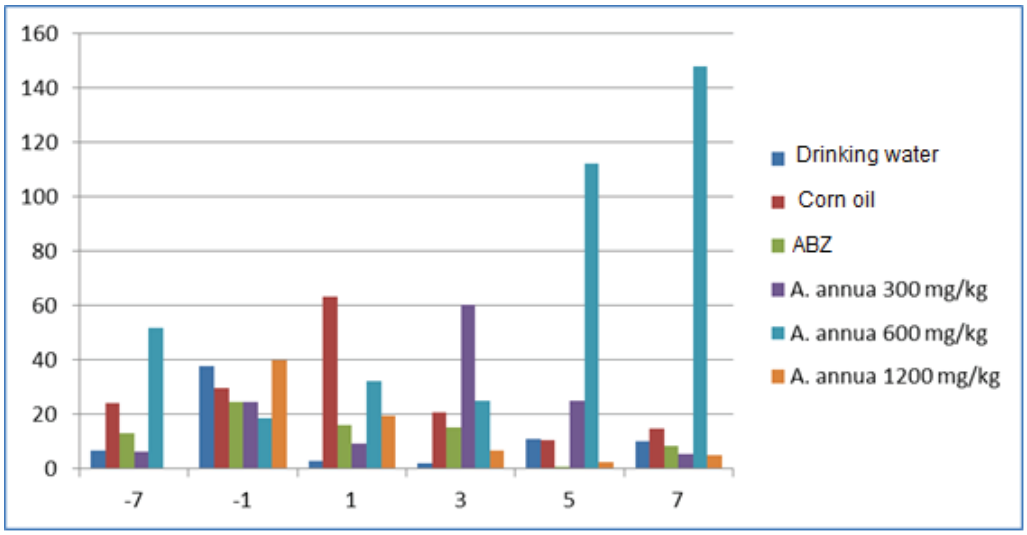

Figure 9. Arithmetic means of *S. obvelata* eggs counted in cellophane tape before application (-7. and -1. days) and during application (1., 3., 5. and 7. days)

In group V, an increase was observed in the average number of eggs from the 7th day until the last day of application. In group IV, when the extract was administered at a dose of 300 mg/kg, increases and decreases followed each other (Figure 9).

Percentage reduction, indicative of effectiveness against oxyurid nematodes, was calculated as follows:

% reduction = 100 x ((I-F) / I)

Where "I" is the arithmetic mean of the parasite eggs in the initial case and "F" is the arithmetic mean in the final state. The arithmetic means of the egg count on the last day decreased by 77.55% compared with the 1st day. In group IV, a continuous decrease was observed from the first day of the application, unlike in group V. A similar situation was observed in Group VI, in which the extract was administered at a dose of 1200 mg/kg. Continuous decreases from the 1st day to the last day followed a slight increase. However, an 88% decrease was determined when comparing the last day's average with that of the 1st day. A similar situation to groups IV and VI was observed in group III, in which ABZ was administered at a dose of 5 mg/kg for three consecutive days, and the average number of eggs decreased continuously from the 1st to the 7th day. Despite the increase observed on the last day, compared to the 1st day, a decrease of 65.58% was determined. The most interesting finding in the *in vivo* experiment results is the decrease in the average number of eggs in the group given drinking water. Compared to the 1st day, there was a 73.47% decrease in the last day's average. This reduction was 50.84% in the corn oil solvent control group.

The *S. obvelata* taxonomy is given in Table 3. The importance of this nematode is due to its widespread presence in laboratory mice and rats and its ability to transmit the disease to humans.

In silico docking studies on the anthelmintic action mechanism of active compounds in plants is an essential first step in developing new anthelmintics. This study is the first to show the antinematodal effect of some active compounds in *A. annua* L. on nematode β-tubulin protein and rat CPT II enzyme by the *in silico* molecular modelling method. Our study's *in silico* docking results showed that the ΔG values of seven of the components we used (quercetin, artemisinin, deoxyartemisinin, friedelin, arteannuin B, stigmasterol, and scopoletin) were more significant than -8 kcal/mol for β-tubulin. With these results, it can be predicted that the binding affinities of the above molecules to the nematode β-tubulin protein are low. These docking results are considered to be reliable since

Table 3. Taxonomy of Oxyurid species *S. obvelata* on which the antinematodal effect of *A. annua* L. n-hexane extract was tested.

Parasite	*Syphacia obvelata* Rudolphi, 1802 (F: Oxyuridae Cobbold, 1864)
Host type	Laboratory mouse *Mus musculus* Linnaeus (1758) (F: Muridae)
Infection site	Small intestine, cecum, colon, and anal opening
Locality type	Bursa Uludağ University Experimental Animal Center, Bursa
The place where the samples are kept	Bursa Uludağ University Faculty of Science and Literature Biology Department Parasitology Laboratory

the RMSD value was below 2 Å (RMSD = 1.56 Å) according to the redocking results of β-tubulin and its natural ligand Albendazole. The K_i values in the table indicate that the antinematodal effects of these molecules may occur in a way independent of the inhibition of β-tubulin. The results of docking performed with the rnCPT II enzyme support this estimate. It has come to our attention that the branched-chain in the ligand's cyclopentane ring plays an important role in the positioning of stigmasterol in the CPT II. In particular, the occurrence of alkyl interactions between the branched-chain of stigmasterol and the surrounding residues (LEU592, PHE602, MET135, GLY600 and ALA613) of the α-helix increased the affinity (Figure 6B). The docking results of arteannuin B and scopoletin showed that only these two molecules out of nine molecules had a higher affinity for β tubulin. While arteannuin B binds to both proteins with high affinity, the value with β tubulin was found to be at a very successful level of -10.68 kcal/mol. This result suggests that arteannuin B is also a highly potent anthelmintic drug candidate. Although it was understood that both friedelin and stigmasterol were not blood-brain barrier permeable according to the SwissADME results, this is not important since our study investigated the effects on nematodes in the gastrointestinal (GI) system. These two molecules are poorly soluble in water and it has been shown that they must be taken with other solvents. Corn oil was used as a solvent since the n-hexane extract appeared to be insoluble in water and DMSO in the *in vivo* experiment. Therefore, it can be predicted that these two molecules may be dissolved in oil. However, since the molecules are not isolated from the n-hexane extract by chromatography, nothing definite can be said. Tubulin protein, which is the target of ABZ, is a protein that forms the cytoskeleton found in all organisms. Therefore, its inhibition can cause side effects. The fact that stigmasterol and friedelin, the molecules tested in this study, inhibit CPT II instead of β-tubulin is promising for the discovery of fewer side-effect drugs than ABZ. In some important studies that investigated the active compounds in plants in terms of anthelmintics by *in silico* methods, predictions have been made about herbal ligands' activities. The theoretical structure of beta-tubulin, which we used in our study, was used in the molecular docking experiment of Satyendra et al. [36] to assess some derivative molecules' anthelmintic effects. In another study, components such as ellagic acid, quercetin, isoquercetin, and caffeic acid found in medicinal plants of *Achyrocline satureioides* were isolated, and caffeic acid was investigated *in silico* and *in vitro* methods in terms of antioxidant and toxicological activities. As a result, *in silico* prediction of quercetin, isoquercetin, and caffeic acid showed the probability of low toxic risk [37].

Some previous experimental studies have revealed the anthelmintic effects of various plant extracts on oxyurides. Gogoi and Yadav [38] demonstrated the *in vivo* and *in vitro* anthelmintic effect of *Caesalpinia bonducella* on *S. obvelata*. When investigated via the anal band and faecal examination, *C. bonducella* extract resulted in a 41% reduction of *S. obvelata* eggs in naturally infected mice and a 93% faster paralysis and consequently the death of *S. obvelata* adults *in vitro*. According to research on the anthelmintic effect of *Verbascum* species on oxyurids in naturally infected laboratory mice from Türkiye, 100 mg/kg doses of *V. lasianthum, V. latisepalum, V. mucronatum* and *V. salviifolum* extracts were not effective as a 0.5 mg/kg dose of Fenbendazole [39]. In a study by de Amorin et al. [40], latexes of two different fig species were investigated in terms of their anthelmintic effects against *S. obvelata*, *A. tetraptera,* and *Vampirolepis nana*. When latex obtained from *Ficus inspida* Willd. was given orally to naturally infected mice for three consecutive days, it killed 38.6 % of nematodes in the gastrointestinal system. Although fig is known as an anthelmintic herb in folkloric medicine, this study revealed insufficient anthelmintic activity of *Ficus inspida* latex. The fact that latex has a weak anthelmintic effect despite its high acute toxicity and haemorrhagic enteritis shows that it would be more appropriate not to use the plant's latex for this purpose. In our study, it can be said that the 1200 mg/kg dose of *A. annua* L. n-hexane extract had an anthelmintic effect on *S. obvelata*, and the 5 mg/kg dose of ABZ did not have a significant impact when compared with the drinking water control group. Since the most commonly used antinematodal drugs in the market are generally broad-spectrum, the plants can be used for this purpose from the same perspective. This study shows that *A. annua* L. has a general effect on nematodes in the gastrointestinal system.

When the fresh or cold dried materials of *A. annua* L. are analysed in terms of nutritional and antioxidant effects, it is obvious that it will be beneficial to include them in the diets of human and breeding animals due to the presence of elements such as minerals, amino acids, iron, zinc, sodium and vitamin E [41]. This herb contains a reasonably high amount of essential amino acids, of which amino acids such as isoleucine, lysine, and tryptophan are higher than the standard amounts recommended for preschool children according to WHO data [42]. Moreover, the plant is rich in vitamin E as well as antioxidants and flavonoids such as quercetin [43]. The potential antioxidant activity of *A. annua* L. leaf extracts has positive effects on human health. Chukwurah et al. [44] demonstrated that 70% ethanolic extracts of *A. annua* L. leaves have higher antioxidant activity than 100% ethanolic extract *in vitro*. According to this study, the antioxidant activity of the extracts is high considering the hydroxyl, nitric oxide, and hydrogen peroxide radical scavenging activities. In particular, hydroxyl scavenging activity was found to be above standards (IC50 = 2.39-3.81 mg/mL), and it was also found to be excellent (79.81% -86.70%) on lipid peroxidation [44]. A study on sheep infected with *Haemochus contortus* showed that oral administration of the *A. annua* L. aqueous extract and artemisinin obtained from this plant had a low-level anthelmintic effect [22]. In sheep infected with *Fasciola hepatica*,

a single dose of 40 mg/kg (iv) of artesunate from *A. annua* L. reduced the egg count by 69% and the worm count by 77%. The same application of artemether obtained from the same plant reduced the number of eggs by 97.6% and the number of worms by 91.9% [45]. Extracts of *A. annua* L. were found to be 81.6–83.2% inhibitory against *Cryptosporidium parvum* in mice [46]. Our study's *in silico* experiment showed that the anthelmintic effect of artemisinin would be weak according to the K_i values which were 6.37 μM for β-tubulin protein and 255.16 nM for CPT II enzyme. Also, quercetin was not found as an important inhibitor in these ligands according to ΔG values. Vijayakumar et al. (2020) had shown that quercetin binds to SARS-CoV-2 target spike (S) protein with -7.8 kcal/mol free energy of binding *in silico*. Hence it had been suggested as an antiviral affected flavonoid [47]. In the present study, the binding affinity of quercetin to the anthelmintic target protein was found lower.

CONCLUSION

In conclusion, to discover drugs with fewer side effects, it will be useful to evaluate this study's results from different angles and especially to include stigmasterol *in vitro* and *in vivo* experiments. The illustrations of possible chemical interactions in this study not only aimed to predict interactions at the atomic level but also to highlight the importance of the structure-activity relationship in anthelmintic drug development. One of the most critical conclusions from the study is that a bulky side chain substituted with cyclopentane in the steroid ring directly affects the CPT II binding site's affinity. Additionally, stigmasterol and friedelin, which have a large core due to the union of at least four rings, need a slightly large cavity to settle in the protein, thus preventing its positioning in β-tubulin. This result provides new data that could be evaluated to discover alternative drugs with fewer side effects than ABZ. Docking analyses of stigmasterol and friedelin support this, and K_i values for the CPT II enzyme were calculated to be 9.43 nM and 13.07 nM, respectively. These two components are promising in terms of eliminating nematode species found in the gastrointestinal tract, particularly those that disrupt children's mental and physical development.

Arteannuin-B being a sesquiterpenlacton, is the most successful molecule in the searched ligands, and can be bonded to both anthelmintic target proteins with very low free binding energy. First time in this study anthelmintic feature of arteannuin-B was investigated and showed that it was potent anthelmintic. It is the first study that searched the molecules that can be responsible for the anthelmintic effect of *A. annua* L. with *in silico* docking methods. These results are significant since they showed that arteannuin-B was more potent than artemisinin. Scopoletin is a coumarin derivative followed by arteannuin-B so it can be a promising antinematodal inhibitor. These data might be a starting point for cancer researchers because arteannuin-B and scopoletin can be β-tubulin inhibitors. The probable support of this study to the literature is being understood when it is taken into account that *in silico* studies on the development of herbal ligands-based anthelmintics are very few.

According to the SwissADME results, the GI absorptions of these two components were low, but these properties will have a positive effect by increasing the inhibition against helminths in the GI. Thus, the concentration of these molecules in GI will not be easily reduced, and helminths will be exposed to stigmasterol and friedelin more intensely. It is usual for friedelin in triterpenoid form and stigmasterol in steroid structure to not dissolve in water. These components can be taken with oil-based solvents when taken orally. In the *in vivo* experiment, *A. annua* L. n-hexane extract dissolved in corn oil, when administered at doses of 300 mg/kg and 1200 mg/kg, caused a decrease in the number of *S. obvelata* eggs on the last day of administration, which may be due to stigmasterol and friedelin. The results can be used to discover a new herbal ligand-based anthelmintic molecule and show that these two components are worthy of isolation and investigation in *in vitro* and *in vivo* studies.

ACKNOWLEDGEMENTS

We dedicate this article to our esteemed Prof. Dr. Hulusi Malyer. This article would not have been possible without his support and helpfulness. It affected us deeply that he left this world while this article was being written. His soul rests in peace.

This research did not receive any specific grant from funding agencies in the public, commercial, or not-for-profit sectors.

AUTHORSHIP CONTRIBUTIONS

Authors equally contributed to this work.

DATA AVAILABILITY STATEMENT

The authors confirm that the data that supports the findings of this study are available within the article. Raw data that support the finding of this study are available from the corresponding author, upon reasonable request.

CONFLICT OF INTEREST

The author declared no potential conflicts of interest with respect to the research, authorship, and/or publication of this article.

ETHICS

There are no ethical issues with the publication of this manuscript.

REFERENCES

[1] World Health Organization. Accelerating work to overcome the global impact of neglected tropical diseases: A roadmap for implementation: Executive summary. 2012. Available at: https://apps.who.int/iris/handle/10665/70809. Accessed Feb 7, 2024.

[2] Giray H, Keskinoğlu P. The prevalence of Enterobius vermicularis in schoolchildren and affecting factors. Turkiye Parazitol Derg 2006;30:99–102. [Turkish]

[3] Strelkauskas A, Edwards A, Fahnert B, Pryor G, Strelkauskas J. Microbiology: A clinical approach. 2nd ed. New York: Garland Science; 2015. [CrossRef]

[4] Jacoby RO, Lindsey JR. Risks of infection among laboratory rats and mice at major biomedical research institutions. ILAR J 1998;39:266–271. [CrossRef]

[5] Carty AJ. Opportunistic infections of mice and rats: Jacoby and Lindsey revisited. ILAR J 2008;49:272–276. [CrossRef]

[6] Hedrich HJ. The laboratory mouse. 2nd ed. London, UK: Academic Press, Elsevier; 2012.

[7] Mueller JF. Parasites of Laboratory Animals Robert J. Flynn. J Parasitol 1973;59:835. [CrossRef]

[8] Willcox M, Bodeker G, Geneviève B, Dhingra V, Falquet J, Ferreira JFS, et al. (2004) Artemisia annua as a traditional herbal antimalarial. In: Willcox M, Bodeker G, Rasaoanaivo P, editors. Traditional Medicine, Medicinal Plants and Malaria. Boca Raton: CRC Press; 2004. [CrossRef]

[9] Bora KS, Sharma A. The genus Artemisia: A comprehensive review. Pharm Biol 2011;49:101–109. [CrossRef]

[10] van der Kooy F, Sullivan SE. The complexity of medicinal plants: The traditional Artemisia annua formulation, current status and future perspectives. J Ethnopharmacol 2013;150:1–13. [CrossRef]

[11] Zheng GQ. Cytotoxic terpenoids and flavonoids from Artemisia annua. Planta Med 1994;60:54–57. [CrossRef]

[12] Abad MJ, Bedoya LM, Apaza L, Bermejo P. The artemisia L. Genus: A review of bioactive essential oils. Molecules 2012;17:2542–2566. [CrossRef]

[13] Wang D, Cui L, Chang X, Guan D. Biosynthesis and characterization of zinc oxide nanoparticles from Artemisia annua and investigate their effect on proliferation, osteogenic differentiation and mineralization in human osteoblast-like MG-63 Cells. J Photochem Photobiol B 2020;202:111652. [CrossRef]

[14] Lubbe A, Seibert I, Klimkait T, van der Kooy F. Ethnopharmacology in overdrive: The remarkable anti-HIV activity of Artemisia annua. J Ethnopharmacol 2012;141:854–859. [CrossRef]

[15] Juteau F, Masotti V, Bessière JM, Dherbomez M, Viano J. Antibacterial and antioxidant activities of Artemisia annua essential oil. Fitoterapia 2002;73:532–535. [CrossRef]

[16] Pirali-Kheirabadi Kh, Teixeira da Silva J. In-vitro assessment of the acaricidal properties of artemisia annua and zataria multiflora essential oils to control cattle ticks. Iran J Parasitol 2011;6:58–65.

[17] Nair MS, Huang Y, Fidock DA, Polyak SJ, Wagoner J, Towler MJ, et al. Artemisia annua L. extracts inhibit the in vitro replication of SARS-CoV-2 and two of its variants. J Ethnopharmacol 2021;274:114016. [CrossRef]

[18] Faurant C. From bark to weed: The history of artemisinin. Parasite 2011;18:215–218. [CrossRef]

[19] Shukla KL, Gund TM, Meshnick SR. Molecular modeling studies of the artemisinin (qinghaosu)-hemin interaction: Docking between the antimalarial agent and its putative receptor. J Mol Graph 1995;13:215–222. [CrossRef]

[20] Cheng F, Shen J, Luo X, Zhu W, Gu J, Ji R, et al. Molecular docking and 3-D-QSAR studies on the possible antimalarial mechanism of artemisinin analogues. Bioorg Med Chem 2002;10:2883–2891. [CrossRef]

[21] İbn-i Sina. El-kanun fi't-tıbb. (Çev. Kahya E.) Ankara: Atatürk Kültür, Dil ve Tarih Yüksek Kurumu Atatürk Kültür Merkezi; 2010.

[22] Cala AC, Ferreira JF, Chagas AC, Gonzalez JM, Rodrigues RA, Foglio MA, et al. Anthelmintic activity of Artemisia annua L. extracts in vitro and the effect of an aqueous extract and artemisinin in sheep naturally infected with gastrointestinal nematodes. Parasitol Res 2014;113:2345–2353. [CrossRef]

[23] National Library of Medicine. Friedelin. Available at: https://pubchem.ncbi.nlm.nih.gov/compound/Friedelin. Accessed Feb 11, 2021.

[24] National Library of Medicine. Stigmasterol. Available at: https://pubchem.ncbi.nlm.nih.gov/compound/Stigmasterol. Accessed Feb 11, 2021.

[25] Morris GM, Goodsell DS, Halliday RS, Huey R, Hart WE, Belew RK, et al. Automated docking using a Lamarckian genetic algorithm and empirical binding free energy function. J Comput Chem 1998;19:1639–1662. [CrossRef]

[26] Taylor CM, Wang Q, Rosa BA, Huang SC, Powell K, Schedl T, et al. Discovery of anthelmintic drug targets and drugs using chokepoints in nematode metabolic pathways. PLoS Pathog 2013;9:e1003505. [CrossRef]

[27] Huey R, Morris GM, Olson AJ, Goodsell DS. A semiempirical free energy force field with charge-based desolvation. J Comput Chem 2007;28:1145–1152. [CrossRef]

[28] Morris GM, Huey R, Lindstrom W, Sanner MF, Belew RK, Goodsell DS, et al. AutoDock4 and AutoDockTools4: Automated docking with selective receptor flexibility. J Comput Chem 2009;30:2785–2791. [CrossRef]

[29] Dassault Systèmes. BIOVIA, Discovery Studio Modeling Environment, Release 2020, San Diego: Dssault Systèmes 2020. Available at: https://www.3ds.com/products-services/biovia/. Accessed Feb 8, 2024.

[30] Robinson MW, McFerran N, Trudgett A, Hoey L, Fairweather I. A possible model of benzimidazole binding to beta-tubulin disclosed by invoking an inter-domain movement. J Mol Graph Model 2004;23:275–284. [CrossRef]

[31] Hsiao YS, Jogl G, Esser V, Tong L. Crystal structure of rat carnitine palmitoyltransferase II (CPT-II). Biochem Biophys Res Commun 2006;346:974–980. [CrossRef]

[32] Sterling T, Irwin JJ. ZINC 15--ligand discovery for everyone. J Chem Inf Model 2015;55:2324–2337. [CrossRef]

[33] Kim S, Chen J, Cheng T, Gindulyte A, He J, He S, et al. PubChem in 2021: New data content and improved web interfaces. Nucleic Acids Res 2021;49:D1388–D1395. [CrossRef]

[34] O'Boyle NM, Banck M, James CA, Morley C, Vandermeersch T, Hutchison GR. Open Babel: An open chemical toolbox. J Cheminform 2011;3:33. [CrossRef]

[35] Daina A, Michielin O, Zoete V. SwissADME: A free web tool to evaluate pharmacokinetics, drug-likeness and medicinal chemistry friendliness of small molecules. Sci Rep 2017;7:42717. [CrossRef]

[36] Satyendra RV, Vishnumurthy KA, Vagdevi HM, Rajesh KP, Manjunatha H, Shruthi A. Synthesis, in vitro antioxidant, anthelmintic and molecular docking studies of novel dichloro substituted benzoxazole-triazolo-thione derivatives. Eur J Med Chem 2011;46:3078–3084. [CrossRef]

[37] Salgueiro AC, Folmer V, da Rosa HS, Costa MT, Boligon AA, Paula FR, et al. In vitro and in silico antioxidant and toxicological activities of Achyrocline satureioides. J Ethnopharmacol 2016;194:6–14. [CrossRef]

[38] Gogoi S, Yadav AK. In vitro and in vivo anthelmintic effects of Caesalpinia bonducella (L.) Roxb. leaf extract on Hymenolepis diminuta (Cestoda) and Syphacia obvelata (Nematoda). J Intercult Ethnopharmacol 2016;5:427–433. [CrossRef]

[39] Kozan E, Çankaya IT, Kahraman C, Akkol EK, Akdemir Z. The in vivo anthelmintic efficacy of some Verbascum species growing in Turkey. Exp Parasitol 2011;129:211–214. [CrossRef]

[40] de Amorin A, Borba HR, Carauta JP, Lopes D, Kaplan MA. Anthelmintic activity of the latex of Ficus species. J Ethnopharmacol 1999;64:255–258. [CrossRef]

[41] Brisibe EA, Umoren UE, Brisibe F, Magalhães PM, Ferreira JFS, Luthria D, et al. Nutritional characterisation and antioxidant capacity of different tissues of Artemisia annua L. Food Chem 2009;115:1240–1246. [CrossRef]

[42] Noack R. Energy and protein requirements. Report of a Joint FAO/WHO Ad Hoc Expert Committee. WHO Technical Report Series No. 522, 118 S., Genf 1973. Food/Nahrung 1973;18:329–332. [CrossRef]

[43] Bahorun T, Luximon-Ramma A, Crozier A, Aruoma OI. Total phenol, flavonoid, proanthocyanidin and vitamin C levels and antioxidant activities of Mauritian vegetables. J Sci Food Agric 2004;84:1553–1561. [CrossRef]

[44] Chukwurah PN, Brisibe EA, Osuagwu AN, Okoko T. Protective capacity of Artemisia annua as a potent antioxidant remedy against free radical damage. Asian Pac J Trop Biomed 2014;4(Suppl 1):S92–98. [CrossRef]

[45] Keiser J, Veneziano V, Rinaldi L, Mezzino L, Duthaler U, Cringoli G. Anthelmintic activity of artesunate against Fasciola hepatica in naturally infected sheep. Res Vet Sci 2010;88:107–110. [CrossRef]

[46] Youn HJ, Noh JW. Screening of the anticoccidial effects of herb extracts against Eimeria tenella. Vet Parasitol 2001;96:257–263. [CrossRef]

[47] Vijayakumar BG, Ramesh D, Joji A, Jayachandra Prakasan J, Kannan T. In silico pharmacokinetic and molecular docking studies of natural flavonoids and synthetic indole chalcones against essential proteins of SARS-CoV-2. Eur J Pharmacol 2020;886:173448. [CrossRef]